doi:10.1093/brain/awu102 Brain 2014: 137; 2015–2026 | 2015

BRAIN
A JOURNAL OF NEUROLOGY

Directional deep brain stimulation: an intraoperative double-blind pilot study

Claudio Pollo,[1] Alain Kaelin-Lang,[2] Markus F. Oertel,[1] Lennart Stieglitz,[1] Ethan Taub,[3] Peter Fuhr,[4] Andres M. Lozano,[5] Andreas Raabe[1] and Michael Schüpbach[2]

1 Department of Neurosurgery, Bern University Hospital, Inselspital, Bern, Switzerland
2 Department of Neurology, Bern University Hospital, Inselspital, Bern, Switzerland
3 Department of Neurosurgery, Basel University Hospital, Basel, Switzerland
4 Department of Neurology, Basel University Hospital, Basel, Switzerland
5 Department of Neurosurgery, Toronto Western Hospital, University of Toronto, Toronto, Canada

Correspondence to: Claudio Pollo, MD,
Department of Neurosurgery,
Bern University Hospital, Inselspital Bern,
Freiburgstrasse, CH-3010 Bern
E-mail: claudio.pollo@insel.ch

See doi:10.1093/brain/awu126 for the scientific commentary on this article.

Deep brain stimulation of different targets has been shown to drastically improve symptoms of a variety of neurological conditions. However, the occurrence of disabling side effects may limit the ability to deliver adequate amounts of current necessary to reach the maximal benefit. Computed models have suggested that reduction in electrode size and the ability to provide directional stimulation could increase the efficacy of such therapies. This has never been demonstrated in humans. In the present study, we assess the effect of directional stimulation compared to omnidirectional stimulation. Three different directions of stimulation as well as omnidirectional stimulation were tested intraoperatively in the subthalamic nucleus of 11 patients with Parkinson's disease and in the nucleus ventralis intermedius of two other subjects with essential tremor. At the trajectory chosen for implantation of the definitive electrode, we assessed the current threshold window between positive and side effects, defined as the therapeutic window. A computed finite element model was used to compare the volume of tissue activated when one directional electrode was stimulated, or in case of omnidirectional stimulation. All but one patient showed a benefit of directional stimulation compared to omnidirectional. A best direction of stimulation was observed in all the patients. The therapeutic window in the best direction was wider than the second best direction ($P = 0.003$) and wider than the third best direction ($P = 0.002$). Compared to omnidirectional direction, the therapeutic window in the best direction was 41.3% wider ($P = 0.037$). The current threshold producing meaningful therapeutic effect in the best direction was 0.67 mA (0.3–1.0 mA) and was 43% lower than in omnidirectional stimulation ($P = 0.002$). No complication as a result of insertion of the directional electrode or during testing was encountered. The computed model revealed a volume of tissue activated of 10.5 mm^3 in omnidirectional mode, compared with 4.2 mm^3 when only one electrode was used. Directional deep brain stimulation with a reduced electrode size applied intraoperatively in the subthalamic nucleus as well as in the nucleus ventralis intermedius of the thalamus significantly widened the therapeutic window and lowered the current needed for beneficial effects, compared to omnidirectional stimulation. The observed side effects related to direction of stimulation were consistent with the anatomical location of surrounding structures. This new approach opens the door to an improved deep brain stimulation therapy. Chronic implantation is further needed to confirm these findings.

Keywords: deep brain stimulation; directional electrode; essential tremor; Parkinson's disease; volume of tissue activated
Abbreviation: DBS = deep brain stimulation

Received November 29, 2013. Revised March 11, 2014. Accepted March 11, 2014. Advance Access publication May 19, 2014

Introduction

Deep brain stimulation (DBS) of different targets has demonstrated the potential to alleviate the symptoms of a variety of neurological conditions, including movement disorders such as Parkinson's disease, essential tremor and dystonia. More recently, DBS has shown some efficacy in treating psychiatric disorders and epilepsy (Lozano and Lipsman, 2013). In advanced Parkinson's disease or essential tremor, DBS applied in the subthalamic nucleus and nucleus ventralis intermedus, respectively, is recognized as a safe and effective therapy for the improvement of symptoms including tremor, rigidity and bradykinesia (Benabid *et al*., 2009). However, because of the restricted size of the functional areas within these structures and the proximity of surrounding structures, stimulation may be limited by the apparition of acute disabling side effects such as tonic muscular contraction, dysarthria, conjugate eye deviation, paraesthesia or gait imbalance (Beric *et al*., 2002; Hariz, 2002; Krack *et al*., 2002; Tripoliti *et al*., 2008). It has also been reported that spillover of stimulation to non-motor portions of the subthalamic nucleus may induce behavioural impairment and limbic side effects such as depression and impulsivity (Stefurak *et al*., 2003; Temel *et al*., 2006). The occurrence of stimulation-related adverse effects is an important limitation of DBS therapies.

Finite-element models of electric field distribution have significantly contributed to a better understanding of the volume of tissue activated surrounding the stimulating electrodes, and have brought new insight when correlating the occurrence of side effects with the position of the activated electrode for each individual situation (Keane *et al*., 2012). In particular, it has been reported that electrode size has an important influence on the occurrence of side effects; therefore, high precision is needed in the placement of electrode leads (Frankemolle *et al*., 2010). This is supported by several studies in which stimulation of the superior and lateral portion of the subthalamic nucleus, which is considered to be the motor part, was found to be correlated with the best clinical efficacy (Rodriguez-Oroz *et al*., 2001; Herzog *et al*., 2004; Godinho *et al*., 2006; Pollo *et al*., 2007). Maks *et al*. (2009) have further suggested that limiting the activated tissue volume to this region improves Unified Parkinson's Disease Rating Scale performance (Maks *et al*., 2009).

Given limitations in electrode size, which translate to inadequate activated tissue volumes, accurate targeting of therapeutic regions in conjunction with avoiding undesirable regions remains challenging, particularly because the placement of the chronically implanted electrodes may be suboptimal.

We hypothesize that a reduction in electrode size and the ability to provide directional stimulation could be advantageous. Reducing the electrode surface area and the ability to steer electrical current would result in a reduction of activated tissue volume, which may improve clinical efficacy of DBS by reaching the expected beneficial effects at a lower current, and in addition could increase the current threshold at which side effects appear. This hypothesis has been theoretically analysed through modelling (Keane *et al*., 2012) and design (Martens *et al*., 2011) of directional DBS devices. However, the proof of concept of directional stimulation has not yet been demonstrated in humans. In the present pilot study, we investigate directional stimulation applied intraoperatively in the subthalamic nucleus and nucleus ventralis intermedus of patients suffering from Parkinson's disease and essential tremor, respectively.

Materials and methods

Patients characteristics and inclusion criteria

A total of 13 patients, 11 with Parkinson's disease (eight males, three females, age 33–72, median 59 years) and two males with essential tremor (age 54 and 67 years), who were selected to undergo DBS at the University Hospital of Bern were included in this study. The study inclusion criteria for patients with Parkinson's disease were: age 18–75 years; established diagnosis of idiopathic Parkinson's disease with motor complications for at least 2 years; a history of at least 30% improvement on the Unified Parkinson's Disease Rating Scale III scale with dopaminergic therapy (except in the tremor-dominant subtype). For patients with essential tremor, inclusion criteria were: age 18–80; established diagnosis of essential tremor for at least 2 years; functional disability due to tremor not adequately controlled by medication for at least 3 months before implantation.

Exclusion criteria were: dementia (a score of $\leqslant$130 on the Mattis Dementia Rating Scale, with scores ranging from 0 to 144 and higher scores indicating better functioning), major depression with suicidal thoughts (a score of >25 on the Beck Depression Inventory II with scores ranging from 0 to 63 and higher scores indicating worse functioning), epilepsy, coagulopathies, presence of an electrical or electromagnetic implant (e.g. cochlear implant, pacemaker), previous surgery for the treatment of Parkinson's disease or essential tremor, any medical or psychological problem that would interfere with the conduction of the study protocol, pregnancy and abuse of drugs or alcohol.

We also excluded patients in which baseline rigidity or tremor significantly decreased or disappeared just before or during the test phase because of micro-lesion effects during surgery.

The study conformed to the Good Clinical Practice guidelines and the International Organization for Standardization 14155 standard. The protocol was approved by the ethics committee of the canton of Bern and by the Swiss Competent Authority. All patients provided written informed consent.

Directional deep brain stimulation device

A DBS lead was designed specifically for the study (directSTNAcute, Aleva Neurotherapeutics SA). It incorporates six directional contacts, with three directional contacts on each of two levels. The directional contacts are each 1 mm $\times$ 1 mm in dimension, with a longitudinal spacing of 0.5 mm. The device also incorporates two omnidirectional electrodes proximal to the directional contacts, which were not used in the course of this study. The device architecture and electrode arrangement are shown in Fig. 1.

Finite element modelling

A 3D Finite Element Model of the directional DBS lead was constructed with the aid of the COMSOL Multiphysics v4.0 software package (COMSOL Inc.). The simulation places the lead in a cylinder

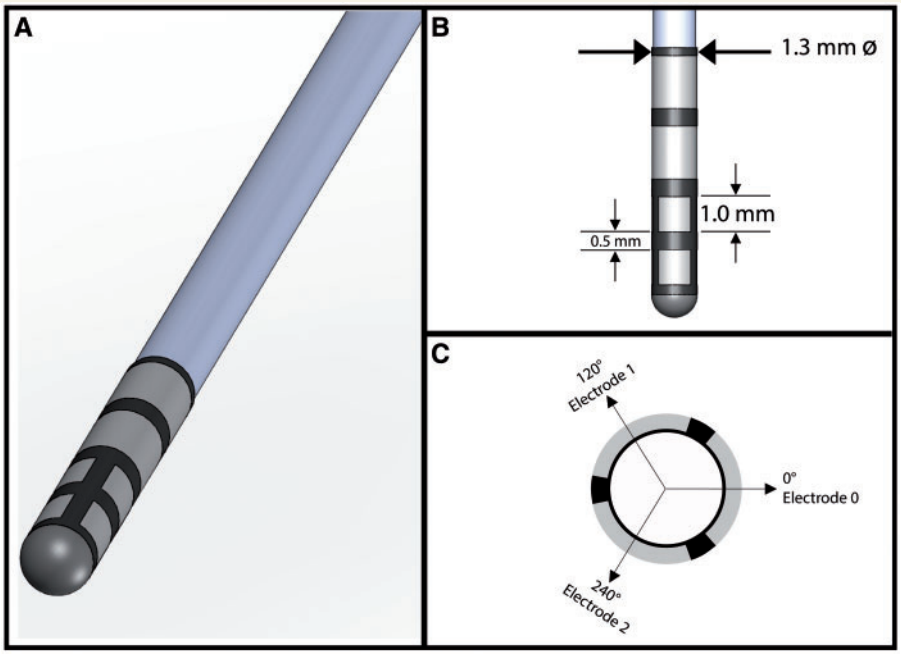

Figure 1 Distal end of the directSTNAcute lead. (**A**) 3D representation. (**B**) Longitudinal view showing the dimensions of the directional electrodes and spacing. (**C**) Axial view with angles of direction.

of diameter 5 cm and height 10 cm. The cylindrical boundary is set to ground while its volume is modelled as an isotropic medium with 0.3 S/m (Grill and Mortimer, 1994). The model can simulate both constant voltage and constant current stimulation modes.

The model compares the electrical potential around the directional DBS lead for two modes: the omnidirectional mode, in which current is applied to all three directional electrodes at one level simultaneously, and the directional mode, in which current is applied to only one directional electrode. By solving the model at a given current injection for both cases, an electric potential in the tissue could be determined and the two situations could be compared. Subsequently, the electric potential was superimposed onto the anatomy of the region surrounding the implantation site. This allowed for a comparison of the electrical fields induced in the two cases, i.e. omnidirectional and directional stimulation, to be performed.

Modelling theory also suggests that calculating the activated tissue volume is a better indicator of stimulation efficiency in anatomical volumes near the electrode site. Following the method of Buhlmann *et al.* (2011), in which the activating function threshold is derived from a Hodgkin-Huxley model, we computed an activated tissue volume by developing a Hessian matrix at each point in the volume surrounding the electrode lead. The maximum absolute eigenvalues of the Hessian matrix were then compared to a voltage strength threshold. Points with eigenvalues greater than the voltage strength threshold were included in the activated tissue volume. The voltage strength threshold can be calculated by the method proposed by Rattay (1986). An activation function threshold is defined as $S = I \cdot r_s$ where I is the applied current threshold, $r_s = 4 \cdot \rho / d$ is the resistivity of the surround tissue with respect to axon diameter, ρ is the resistivity of the axoplasm (70 Ωcm), and d is the diameter of an axon (5.7 μm in this anatomical region) (McIntyre *et al*., 2002). The activation function S can then be compared to previously published values. For example, McIntyre *et al*. (2004) calculated a threshold of ~12 V/cm^2, Buhlmann *et al.* (2011) calculated ~27 V/cm^2, and Martens *et al.* (2011) calculated ~20 V/cm^2. We chose to represent the activated tissue volume as isolines of threshold values surrounding the lead.

Surgical procedure, intraoperative test setup and postoperative localization of electrodes

Preoperative T_1- and T_2-weighted high-resolution magnetic resonance images (3 T) were co-registered with a stereotactic CT (Leksell frame, Elekta) for targeting and planning the implantation trajectories (iPlan, BrainLab)

Intraoperatively, 3-trajectory microelectrode recording (FHC) and clinical testing by semi-macroelectrode stimulation was performed with the Leadpoint system (Medtronic).

Once the trajectory and site of implantation of the permanent lead had been determined for the first hemisphere operated on (the most symptomatic side), the directional electrode was inserted under fluoroscopic control so that the distal directional ring (contact 0,1,2) was at the Z level of the trajectory that had been chosen for clinical testing and the 0° axis plane of the directSTN lead was directed medially (for subthalamic nucleus stimulation) or directed anteriorly (for nucleus ventralis intermedus stimulation).

The proximal end of the directSTN Acute lead was connected to an octopolar extension cable (Model 37081, Medtronic Inc.).

The extension cable was then connected to a dedicated external neurostimulation cart. This cart was developed to pulse any individual directional electrode, or to pulse any combination of two or three electrodes simultaneously. The system features several Osiris Stimulators (Model 504196, Inomed) and includes a custom-made user interface.

The stimulation parameters were current-driven monopolar monophasic pulses, with pulse width 90 μs and frequency 130 Hz.

Five different stimulation configurations were tested: each of the three individual directions; the three directions (0°, 120°, 240°)

together—which we called omnidirectional stimulation; and a configuration in which two directional contacts facing the best direction, one above the other, pulse together.

Upon completion of the test phase, the directSTN Acute lead was removed and the definitive DBS lead implantation resumed (lead model 3389, Medtronic Inc.).

For each patient, a stereotactic post-operative CT scan was performed and co-registered with the preoperative 3D T_2-weighted MRI (iPlan, BrainLab). Furthermore, the anterior commissure–posterior commissure (AC–PC) coordinates of the point for clinical testing were calculated and mapped onto the closest axial slice in the Schaltenbrand atlas templates (Schaltenbrand and Wahren, 1977), and normalized to the intercommissural points.

Stimulation sequences and assessment of patient's reactions

The sequence of stimulation in the three single directions and in the omnidirectional stimulation was determined before the test phase in a randomized fashion, to prevent bias that might arise if an identical sequence were used in all patients. The fifth stimulation configuration (two directional contacts facing the best direction, one above the other) was performed last, as it required knowledge of the directional contact that gave the best clinical results.

The sequence of stimulations was conducted in a double-blinded fashion, unknown to the patient, the neurosurgeon and the neurologist assessing the patient's reactions. The sequence of directions was known only to the neurologist operating the neurostimulators.

All of the patients were operated on by the same surgeon. The same experienced neurologist assessed the intraoperative response of all patients.

The patient's motor symptoms were assessed at baseline before stimulation. The total stimulation current was increased in increments of 0.1-mA steps. As the electrical current was increased, the therapeutic effect on the motor symptoms was graded by the neurologist on a four-point scale: no effect, partial effect, very good partial effect and full effect.

Once the full therapeutic effect was obtained, the neurophysiologist continued to incrementally increase stimulation current until a sustained treatment-limiting side effect arose, such as paraesthesia, dysarthria or focal muscular contraction. These symptoms disappeared as soon as the stimulation was turned off and indicated the upper limit of the therapeutic window for stimulation.

The current required to obtain a meaningful therapeutic effect (full effect on rigidity or very good partial effect on tremor), as well as the side effects encountered, were assessed for the five stimulation configurations. The width of the therapeutic window was defined as the electrical current at which a sustained side effect appeared minus the electrical current at which a meaningful therapeutic benefit was obtained.

The impedance through each directional contact was also measured before and after the test phase, as a confirmation that the stimulation did take place as intended. Adverse events, intraoperative and post-operative, were recorded.

Data analysis

The therapeutic window and the current threshold for therapeutic effect are presented using the average and (min, max) values. The percentiles 0, 25, 50, 75 and 100 are graphed as box plots. The differences between the best directional stimulation and each of the other stimulation configurations were compared.

A *P*-value was calculated using a Wilcoxon signed-rank test for difference in medians, with continuity correction. We rejected the null hypothesis (= no difference) when P-value < 0.05. These calculations were performed with the NCSS9 software package (NCSS-LLC).

Results

Finite element analysis

In Fig. 2, we show a comparison of stimulation with the directSTN Acute system in omnidirectional and directional modes. The

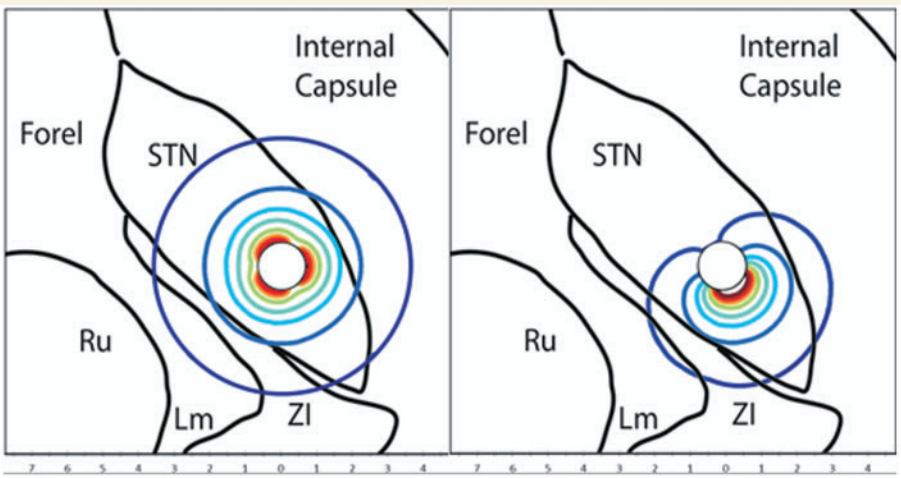

Figure 2 Axial projection of two stimulation modes using Finite Element Analysis and superposition of electric potential onto anatomy adapted from the Schaltenbrand and Wahren atlas, Plate 54 Hv = −3.5. *Left*: All three electrodes simultaneously activated with a total applied current of 3 mA (1 mA per contact). *Right*: Postero-lateral directional electrode active with an applied current of 1.8 mA, avoiding the internal capsule. Horizontal scale represents the distance from the centre of the lead in mm. STN = subthalamic nucleus; ZI = zona incerta; Lm = Lemniscus medialis; Ru = nucleus Ruber; Forel = Forel field.

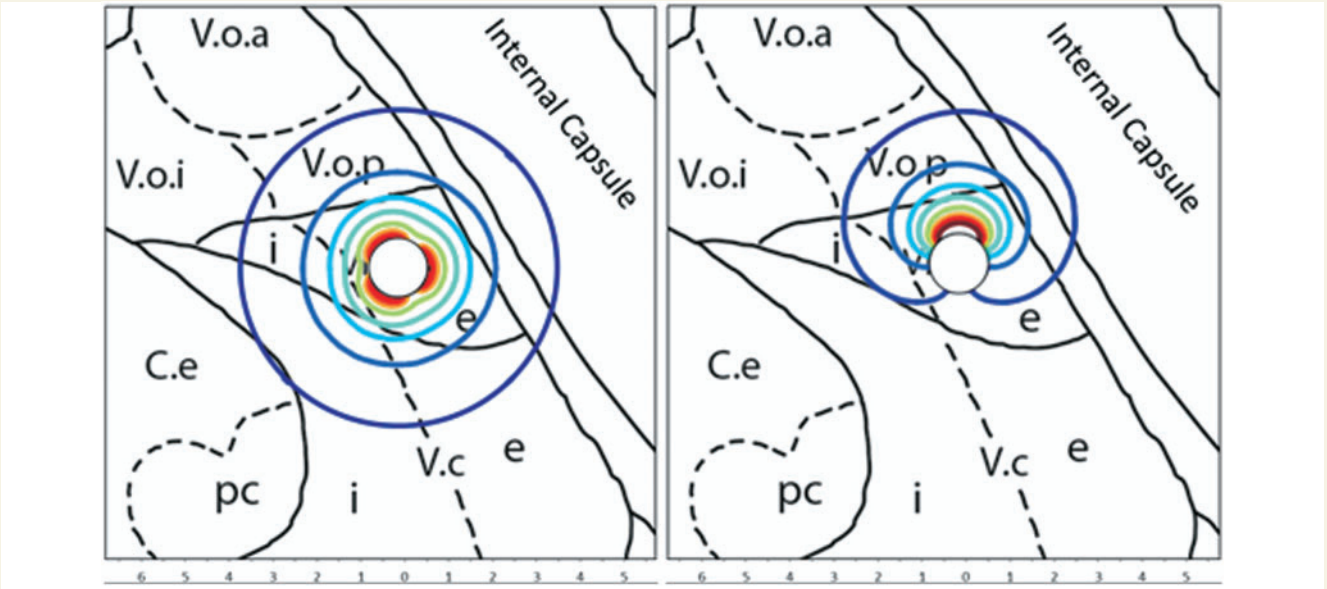

Figure 3 Anatomical representation in the axial projection of region surround the nucleus ventralis intermedus implantation site adapted from the Schaltenbrand and Wahren atlas, Plate 53 Hd = +2. *Left*: All three electrodes simultaneously activated with a total applied current of 3 mA (1 mA per contact). *Right*: Anterior directional electrode active with an applied current of 1.8 mA, avoiding the sensory thalamus. The horizontal scale represents the distance from the centre of the lead in mm. e = externus; i = internus; pc = parvocellularis; C.e = nucleus centralis externus; V.c = nucleus ventralis caudalis; V.o.p = nucleus ventralis oralis posterior; V.o.a = nucleus ventralis oralis anterior; V.o.i = nucleus ventralis oralis internus.

electrical potential is aligned with the anatomy believed to be surrounding the lead during implantation. The iso-potential lines are represented with colours where a darker colour represents a lower iso-potential. The clinically relevant superior and lateral section of the subthalamic nucleus has an applied electric potential in both cases, whereas in the single directional contact case the internal capsule is avoided.

In Fig. 3, we show an analogous comparison of stimulation in the unidirectional and omnidirectional modes superimposed on the anatomy of the nucleus ventralis intermedus, which was the target used for the essential tremor patients. Here, it is apparent that an electric potential directed anteriorly will avoid regions of the sensory thalamus.

The graphs in Fig. 4 represent the calculated isolines of the activated tissue volume, with a comparison of omnidirectional and directional stimulation modes. Calculations were performed with a stimulation voltage of 1 V on the electrodes, meaning that the current delivered in the omnidirectional mode (three electrodes activated) is three times higher than the current delivered in directional mode. The computation reveals that, when the activated tissue volume threshold is set at 12 V/cm^2, a volume of 10.5 mm^3 is activated in omnidirectional mode, whereas a volume of 4.2 mm^3 is activated with a unidirectional electrode.

Therapeutic effects, side effects and correlation with spatial location

The directional test phase lasted 49 min on average, of which 28 min were taken up by the stimulation sequences.

Once the directSTN lead had been inserted at the target site, a rest period of 7 min on average took place before baseline assessment, and the rest period between two stimulation sequences was 2 min on average.

The omnidirectional configuration was the first one tested for four patients and was either in second, third or fourth tested sequence for the other nine patients. Therapeutic effects and side effects were detectable in all five stimulation configurations, but at different electrical current values. A meaningful therapeutic effect was defined as: 'full effect' on reduction of rigidity, or 'very good partial effect' on reduction of tremor. The first sustained side effect encountered, as current was increased, was either dysarthria, focal muscular contraction, or paraesthesias. These side effects are listed for each patient in Tables 1 and 2.

An image parallel to the AC–PC plane was performed at the Z level of the planned trajectory and provides the actual position in relation to the subthalamic nucleus (visible on T_2-weighted images) and nucleus ventralis intermedus (not visible on T_2-weighted images). These images are shown in Tables 1 and 2. The mean (±SD) AC–PC coordinates of the intraoperatively stimulated point were: lateral: 11.71 mm (±1.04), anteroposterior: −2.60 mm (±0.68), vertical: −3.16 mm (±0.67), related to the midcommissural point. Negative anteroposterior and vertical values were posterior and inferior to the midcommissural point, respectively. The map of the stimulated points and mean stimulated point are shown in Fig. 5, provided that it represents an approximation of the reality.

One of the directions gave a higher therapeutic window than the other two directions for every patient. The best direction (best = resulting in the widest directional therapeutic window)

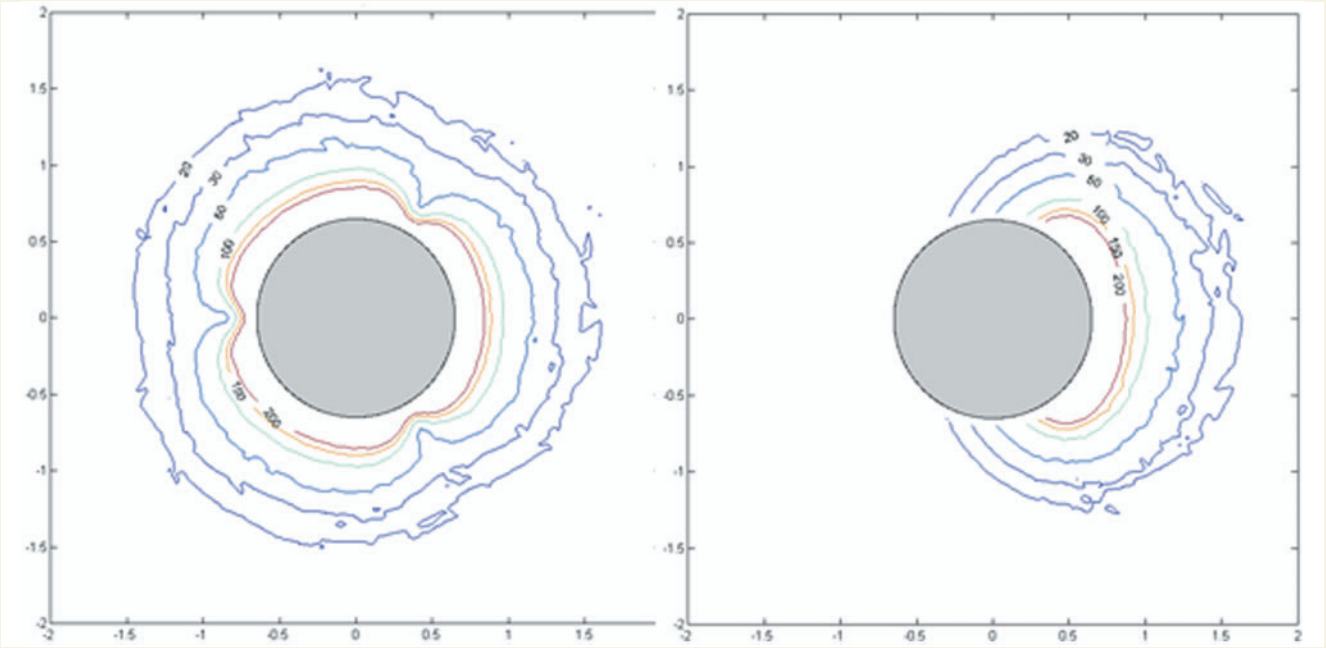

Figure 4 Transverse view of activated tissue volume isolines, when 1 -V stimulation is applied. *Left*: All three electrodes simultaneously activated. *Right*: One-directional electrode activated. The disc represents a cross-section of the lead. The *x*- and *y*-axis labels represent millimetres from the centre of the lead.

Table 1 Directional stimulation in the subthalamic nucleus for patients with Parkinson's disease

Patient's disease	First sustained side effect	Position of the STN electrode at the stimulated point	Best directional therapeutic window		Second best directional therapeutic window		Third best directional therapeutic window	
			Direction	Current producing side effect (mA)	Direction	Current producing side effect (mA)	Direction	Current producing side effect (mA)
PD	Dysarthria	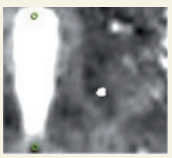	Medial	3.3	Antero-lateral	3.2	Postero-lateral	2.5
PD	Dysarthria	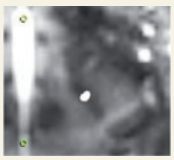	Medial	1.5	Postero-lateral	0.8	Antero-lateral	0.7
PD	Dysarthria	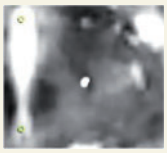	Medial	Above 3.4	Antero-lateral	3.3	Postero-lateral	2.3

(continued)

Table 1 Continued

Patient's disease	First sustained side effect	Position of the STN electrode at the stimulated point	Best directional therapeutic window		Second best directional therapeutic window		Third best directional therapeutic window	
			Direction	Current producing side effect (mA)	Direction	Current producing side effect (mA)	Direction	Current producing side effect (mA)
PD	Dysarthria	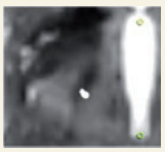	Medial	Above 2.8	Antero-lateral	2.0	Postero-lateral	1.7
PD	Facial contraction	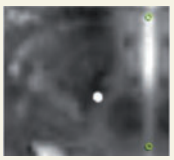	Medial	3.4	Postero-lateral	2.7	Antero-lateral	2.8
PD	Facial contraction	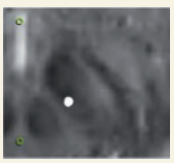	Medial	3.3	Antero-lateral	3.0	Postero-lateral	2.3
PD	Dysarthria	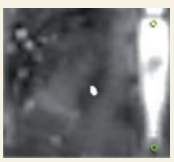	Postero-lateral	3.3	Medial	3.2	Antero-lateral	1
PD	Dysarthria	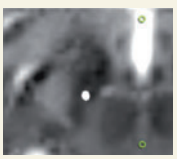	Postero-lateral	2.1	Antero-lateral	2.7	Medial	2.6
PD	Dysarthria	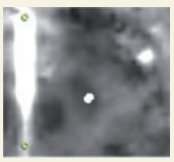	Antero-lateral	2.5	Postero-lateral	1.9	Medial	2.2
PD	Hand paraesthesias	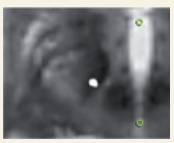	Antero-lateral	above 3.4	Medial	3.3	Postero-lateral	2.7
PD	Leg and foot paraesthesias	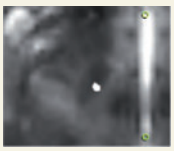	Antero-lateral	2.7	Medial	2.6	Postero-lateral	1

The position of the lead at the level of the tested directional stimulation in the AC–PC referential, the sustained side effects and the currents producing them, according to the direction of stimulation, are shown. Green circles: projection of AC and PC; PD = Parkinson's disease.

Table 2 Directional stimulation in the nucleus ventralis intermedus for patients with essential tremor

Patient's disease	First sustained side effect	Position of the Vim electrode at the stimulated point	Best directional therapeutic window		Second best directional therapeutic window		Third best directional therapeutic window	
			Direction	Current producing side effect (mA)	Direction	Current producing side effect (mA)	Direction	Current producing side effect (mA)
ET	Facial paresthesia	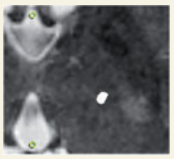	Anterior	2.0	Postero-lateral	1.3	Postero-medial	0.6
ET	Dysarthria	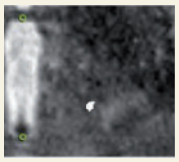	Anterior	1.9	Postero-lateral	1.5	Postero-medial	1.5

The position of the lead at the level of the tested directional stimulation in the AC–PC referential, the sustained side effects and the currents producing them, according to the direction of stimulation, are shown. Green circles: projection of AC and PC; ET = essential tremor.

varied from patient to patient. The other two single directions were designated as second-best and third-best. The directions are presented in Tables 1 and 2.

Nine of 11 subthalamic nucleus patients had motor side effects (seven dysarthria and two muscular contractions) as their first sustained side effect. Six of these nine patients had the best directional therapeutic window in the medial direction, two in the postero-lateral and one in the antero-lateral direction.

The other two subthalamic nucleus patients had paraesthesia as a first sustained side effect, and their best directional therapeutic window was antero-lateral. These two patients had a lateral electrophysiological trajectory $\geqslant$4 mm inside the subthalamic nucleus.

The two nucleus ventralis intermedus patients had the best direction in the anterior direction, and the third-best direction in the postero-medial direction. Both patients had a lateral microrecording trajectory $\geqslant$4 mm inside the nucleus ventralis intermedus.

The observed first sustained side effects were correlated with the direction of stimulation, as shown in Fig. 5.

Therapeutic window

The therapeutic window was measured for each of the stimulation configurations on 12 patients (omnidirectional stimulation was not possible in one patient because of apparition of confusional state).

The therapeutic window in the best direction (i.e. the one that resulted in the widest directional therapeutic window) was 1.93 mA on average (range 1.0–2.9 mA). The therapeutic window in the second-best direction was 1.43 mA on average (0.2–2.9 mA) which was significantly smaller than in the best direction ($P = 0.003$). With an average of 0.96 mA (0–2.1 mA), the worst direction (or third-best) was also significantly lower than the second-best direction ($P = 0.002$). The omnidirectional therapeutic window average was 1.36 mA (range 0.15–3.15 mA). The average therapeutic window in the best direction is 41.3% wider than the omnidirectional therapeutic window ($P = 0.037$), and with a narrower spread of values.

In one patient with tremor-dominant Parkinson's disease, we found no advantage of directional stimulation over omnidirectional stimulation (omnidirectional therapeutic window = 3.15 mA, which was greater than the therapeutic window in any of the three individual directions).

Stimulation of two electrodes simultaneously—the best electrode and the one above it—did not increase the therapeutic window compared to stimulation of the best electrode alone. A representation of the omnidirectional therapeutic window and each single direction is shown in Fig. 6.

Electrical current producing meaningful therapeutic effect

The therapeutic current was measured for each of the stimulation configurations, on 13 patients. As shown in Fig. 7, the average current threshold in the best direction (best = resulting in the best directional therapeutic window) was 0.67 mA (range 0.3–1.0 mA). The average current thresholds in the second-best and worse directions (0.87 mA and 0.92 mA, respectively) did not differ statistically from the current threshold in the best direction.

We note that the best direction current threshold was $\leqslant$ 1.0 mA for all patients, with the narrowest spread of values. The average current threshold for omnidirectional stimulation was 1.17 mA (range 0.6–1.95 mA). The average therapeutic current in the best direction is 43% lower than the omnidirectional one ($P = 0.002$). We note that the best direction threshold current was larger than the omnidirectional threshold current in all 13 patients.

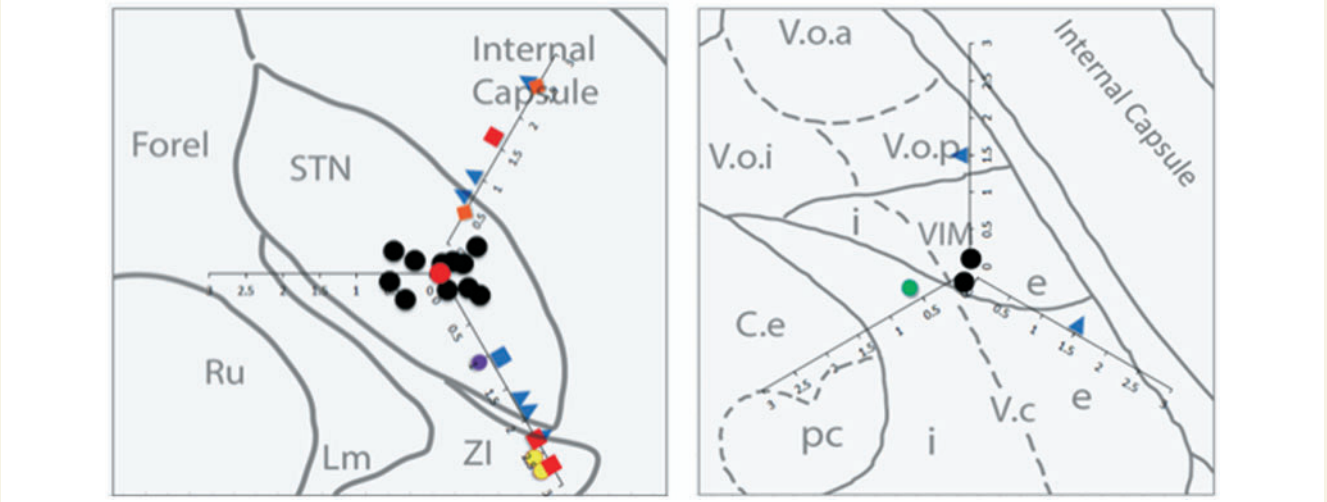

Figure 5 Sustained side effects obtained at the lowest current threshold (mA) according to the direction of stimulation. *Left*: Map of the stimulated points (black dots) and mean stimulated point (red dot) in the subthalamic nucleus with medial, antero-lateral and postero-lateral directions. *Right*: Map of the stimulated points (black dots) in the nucleus ventralis intermedus with anterior, postero-lateral and postero-medial directions, Dysarthria (blue triangle), muscular contraction face (red square), muscular contraction foot (blue square), paraesthesia face (green dot), paraesthesia hand (yellow dot), paraesthesia lower limb (violet dot), dyskinesia (orange diamond). STN = subthalamic nucleus; ZI = zona incerta; Lm = Lemniscus medialis; Ru = nucleus Ruber; Forel = Forel field; e = externus; i = internus; pc = parvocellularis; C.e = nucleus centralis externus; V.o.p = nucleus ventralis oralis posterior; V.o.a = nucleus ventralis oralis anterior; V.o.i = nucleus ventralis oralis internus.

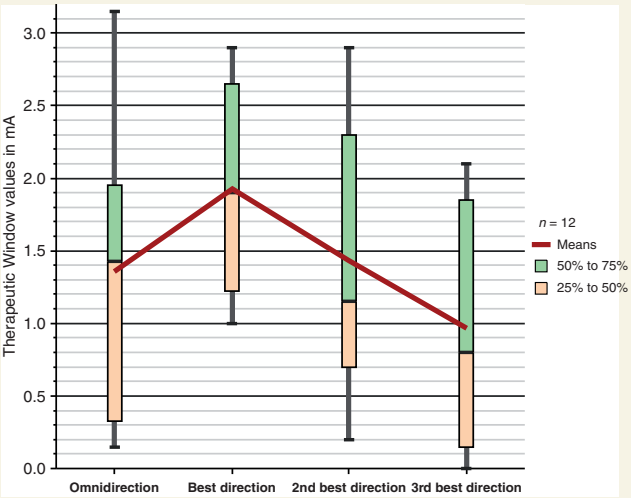

Figure 6 Box plot representing the width of the therapeutic window (percentiles 0, 25, 75, 100), for omnidirectional stimulation and for stimulation in each single direction. Red line = mean therapeutic window.

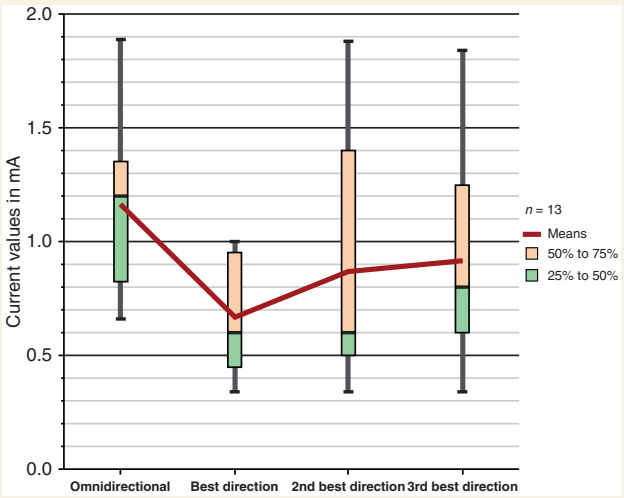

Figure 7 Box plot of the electrical current producing a meaningful therapeutic effect (percentiles 0, 25, 75, 100), for omnidirectional stimulation and stimulation in each single direction. Red line = mean current threshold.

Stimulating two electrodes—the best electrode and the one above it—did not lower the current threshold compared to the best electrode alone.

Adverse effects of directional current testing

No complication due to insertion or stimulation was encountered in the directional test phase.

Discussion

The results of this study indicate that providing directional stimulation in the subthalamic nucleus and nucleus ventralis intermedus with a stimulating electrode of reduced size was able to improve the therapeutic window intraoperatively. To our knowledge this is the first study establishing the proof of concept of directional stimulation in humans.

Directional stimulation with an electrode of reduced size, while allowing a specific orientation and reduction of the activated tissue

volume, provides a new concept of delivering DBS, leading to a more selected activation of the neurons and/or axons surrounding the lead. This enhanced accuracy would be especially desirable in case a DBS lead is not optimally placed, resulting in a reduced intensity of stimulation before the apparition of side effects. Similarly, benefits would likely be achieved in other small and complex target regions where a reduced and directional activated tissue volume may be desirable (Peppe *et al*., 2008), such as the pedunculopontine nucleus (Thevathasan *et al.*, 2011), or other fibre bundle targets, such as the medial forebrain bundle for resistant depression (Schlaepfer *et al*., 2013), the dentato-rubro-thalamic tract for tremor (Coenen *et al*., 2011) or even the zona incerta for Parkinson's disease (Yelnik *et al*., 2003; Plaha *et al*., 2006). Therefore, highly targeted stimulation fields could optimize DBS not only in currently used targets like subthalamic nucleus or nucleus ventralis intermedus, but also in emerging targets and even generate new targets for stimulation.

Previous studies on modelling of the activated tissue volume using directional electrodes have previously emphasized the potential improvement of the therapeutic outcome by avoiding anatomical structures responsible for side effects (Martens *et al*., 2011; Keane *et al*., 2012).

Our Finite Element Model results on directional activated tissue volume in the subthalamic nucleus and nucleus ventralis intermedus, shown in Figs 2 and 3, respectively, represent the situation where lead implantation is ideal and are based on assumption of an individual accuracy of the anatomy surrounding the lead. Nevertheless, they are in accordance with the previous findings, when compared with an omnidirectional lead design. In the case of the nucleus ventralis intermedus DBS, the vicinity of the corticospinal tract in the antero-lateral direction and the sensory thalamus and medial lemniscus in the posterior direction are known to be correlated with motor and sensory side effects, respectively. Similarly, the vicinity of the corticospinal tract in the antero-lateral direction and the medial lemniscus in the posterior direction are also correlated with motor and sensory side effects associated with subthalamic nucleus stimulation.

Our intraoperative observations regarding the type of side effects related to the direction of stimulation are also consistent with the model prediction.

In the subthalamic nucleus, we observed motor side effects, i.e. dysarthria or focal muscular contraction in 9 of 11 patients as a first sustained side effect (Table 1 and Fig. 5). Six of these nine patients had their best direction of stimulation in the medial direction, which provides stimulation away from the corticospinal tract, two in the postero-lateral direction, and only one had its best direction in the antero-lateral direction, showing the shortest distance to the corticospinal tract fibres. Except for two patients, all of them had their worst direction in the lateral direction of stimulation, either antero- or postero-lateral. In Patient 8 (one of the two patients who had medial therapeutic window direction as the worst), we observed that the difference in the current threshold producing dysarthria between medial (2.6 mA) and antero-lateral (2.7 mA) was 0.1 mA. The other (Patient 9) had a higher threshold for appearance of dysarthria in the medial direction (2.2 mA) when compared to the antero-lateral direction (1.9 mA), despite a worse therapeutic window in the last direction explained by a higher current threshold for therapeutic effect.

The antero-lateral direction of stimulation was associated with dyskinesia in 2 of 11 subthalamic nucleus patients. Intraoperative stimulation-induced dyskinesia has been recognized to be encountered in the motor part of the subthalamic nucleus, which has been shown to be located in the superior and lateral portion of the nucleus, as confirmed with electrophysiological data (Rodriguez-Oroz *et al*., 2001), the position of the active electrodes correlated with the best clinical outcome (Godinho *et al*., 2006; Pollo *et al*., 2007), as well as imaging studies (Brunenberg *et al*., 2012; Lambert *et al.*, 2012).

The postero-lateral direction was associated with paraesthesias as a first sustained side effect in 2 of 11 subthalamic nucleus patients, which could be explained by stimulation of the medial lemniscus fibres. In addition, these patients had their best therapeutic window in the antero-lateral direction, whereas the postero-lateral direction was their worst.

Remarkably, as shown in Fig. 5, the medial direction was never associated with a sustained motor or sensitive side effect at the lowest current threshold. We were not able to find a directionally improved therapeutic window compared with omnidirectional stimulation in one patient with tremor-dominant Parkinson's disease. This patient had a resting tremor of fluctuating intensity during the intraoperative testing phase, so that thresholds for stimulation effects were hard to assess reliably.

We were also not able to observe a correlation between the observed best direction therapeutic window and the lead location in relation to the subthalamic nucleus as defined on postoperative imaging resulting from postoperative CT and preoperative T_2-weighted MRI co-registration. This may be explained by the limited number of patients, but also by the image resolution, which does not provide a well delineated subthalamic nucleus in some cases. Finally, the possible errors induced by the co-registration process could also play a role.

In both nucleus ventralis intermedus patients (Table 2), postero-medial direction of stimulation was associated with sustained paraesthesia. This can be explained by the proximity of the sensory nucleus of the thalamus and of the medial lemniscus in these directions. Dysarthria could be elicited in the anterior as well as postero-lateral direction of stimulation. Both nucleus ventralis intermedus patients had their best therapeutic window in the anterior direction, i.e. the direction facing away from the sensory thalamus/medial lemniscus pathways. The current needed for the generation of meaningful therapeutic effects was remarkably low, $\leqslant$1 mA, in all patients.

Intraoperative conditions in terms of tissue reaction to lead insertion (the microlesional effect induced by insertion of the lead and/or surrounding oedema) may differ from those seen in a chronic state. For this reason, intraoperative observations may change over time. To reduce the risk for an oversized intraoperative therapeutic window and the risk of a lowered amount of current needed for beneficial effects induced by these particular conditions, we excluded patients from our study cohort where a microlesion effect was observed after microrecording and/or microstimulation and before directional stimulation testing.

It has been shown that stimulation voltage needs to be increased in the first weeks after implantation to reach the threshold for beneficial as well as side effects. This observation has been correlated with an increase of the impedance at the electrode-tissue interface (Lungu *et al*., 2013).

However, in case of increased impedance, an increase in voltage does not necessitate an increased amount of current to reach the same thresholds, which in turn, does not necessarily correlate with a significant modification of the therapeutic window over time. We performed this intraoperative study using a constant current-based pulse generator, measuring currents delivered in the tissue, whatever the impedance. Similarly, chronically implanted constant-current based generators would better address this issue over time.

Therefore, we suggest that the low amounts of current needed for beneficial effects may also be correlated with the geometry of the electrode as well as its reduced size. This would be expected to increase the local current density, which in turn may promote neural recruitment close to the electrode surface. Thus, a limited activated tissue volume in the motor subthalamic nucleus or nucleus ventralis intermedus may be correlated with a full effect on motor symptoms of Parkinson's disease or essential tremor respectively, as previously suggested by other groups (Maks *et al*., 2009).

With respect to the currently admitted charge density of 30 $\mu C/cm^2$/phase, the maximally allowed amount of current per electrode (surface 1 mm^2) is 3.4 mA with a stimulation at a pulse width of 90 μs. Even if we observed significant beneficial effects at < 1mA in all our patients, and we were able to deliver $\geqslant 3.3$ mA in 6 of 11 patients with Parkinson's disease without observing a subsequent microlesional effect, higher amounts of current may induce potential problems with tissue damage in chronic stimulation.

An increased number of electrodes may result in longer time-requirements with regard to lead programming. The present lead provides a limited number of directional electrodes electrodes to be compatible with the existing implantable impulse generators. On the other hand, the information obtained intra-operatively while determining the best direction therapeutic window may facilitate subsequent programming of the segmented leads. The real time need for optimally programming such electrodes remains to be evaluated.

Our intraoperative test stimulation was limited in time and therefore only a selection of different possible stimulation conditions could be assessed. Moreover, this pilot study included only a small number of patients. Therefore, our acute intraoperative findings remain to be replicated with long-term observations in a clinical study with chronic implantation.

The results depend also on the consistency of the neurologist's clinical judgement and the stability of the patient's symptoms during the testing phase. However, excluding the fluctuation of resting tremor observed in one patient, we found no significant micro-lesion effects before or after insertion of the directional lead. When a transient carry-over effect was present after a testing sequence, the neurologist waited until the reappearance of symptoms before making any new observations.

Conclusion

Intraoperative directional stimulation with a smaller activated tissue volume in the subthalamic nucleus and the nucleus ventralis intermedus significantly widened the therapeutic window for DBS in comparison to omnidirectional stimulation. There were also clear differences in stimulation induced effects depending on the angular orientation of the stimulating electrode contact around the circumference of the electrode shaft. The observed side effects were consistent with the anatomical location of surrounding structures.

Although these results warrant further studies, to confirm the long-term effect of directional stimulation in chronically implanted patients, they clearly suggest that directional stimulation has a strong potential for reducing side effects, widening the therapeutic window, and lowering the therapeutic current. This new approach may open the door to a better DBS therapy, by minimizing the impact of suboptimal lead placement and by prolonging battery life.

Acknowledgements

The authors thank Dr André Mercanzini, PhD for his precious help in providing data concerning finite element model of DBS and Alain Dransart from Aleva Neurotherapeutics, for his precious help in the preparation and realization of the study.

Funding

This study was partially funded by the Swiss Commission for Technology and Innovation (CTI grant number: 10271.1 PFLS-LS). Aleva Neurotherapeutics SA is the sponsor of the clinical study and the provider of the directional leads.

Conflict of interest

Claudio Pollo is co-founder of Aleva Neurotherapeutics.

References

Benabid AL, Chabardes S, Mitrofanis J, Pollak P. Deep brain stimulation of the subthalamic nucleus for the treatment of Parkinson's disease. Lancet Neurol 2009; 8: 67–81.

Beric A, Kelly PJ, Rezai A, Sterio D, Mogilner A, Zonenshayn M, et al. Complications of deep brain stimulation surgery. Stereotact Funct Neurosurg 2002; 77: 73–8.

Brunenberg E, Moeskops P, Backes W, Pollo C, Cammoun L, Vilanova A, et al. Structural and resting state functional connectivity of the subthalamic nucleus: identification of motor STN parts and the hyperdirect pathway. PLoS One 2012; 7: e39061.

Buhlmann J, Hofmann L, Tass PA, Hauptmann C. Modeling of a segmented electrode for desynchronizing deep brain stimulation. Front Neuroeng 2011; 4: 15.

Coenen VA, Mädler B, Schiffbauer H, Urbach H, Allert N. Individual fiber anatomy of the subthalamic region revealed with diffusion tensor

imaging: a concept to identify the deep brain stimulation target for tremor suppression. Neurosurgery 2011; 68: 1069–75.
Frankemolle AMM, Wu J, Noecker AM, Voelcker-Rehage C, Ho JC, Vitek JL, et al. Reversing cognitive-motor impairments in Parkinson's disease patients using a computational modelling approach to deep brain stimulation programming. Brain 2010; 133: 746–61.
Godinho F, Thobois S, Magnin M, Guenot M, Polo G, Benatru I, et al. Subthalamic nucleus stimulation in Parkinson's disease: anatomical and electrophysiological localization of active contacts. J Neurol 2006; 253: 1347–55.
Grill WM, Mortimer JT. Electrical properties of implant encapsulation tissue. Ann Biomed Eng 1994; 22: 23–33.
Hariz MI. Complications of deep brain stimulation surgery. Mov Disord 2002; 17(Suppl 3): S162–166.
Herzog J, Fietzek U, Hamel W, Morsnowski A, Steigerwald F, Schrader B, et al. Most effective stimulation site in subthalamic deep brain stimulation for Parkinson's disease. Mov Disord 2004; 19: 1050–99.
Keane M, Deyo S, Abosch A, Bajwa JA, Johnson MD. Improved spatial targeting with directionally segmented deep brain stimulation leads for treating essential tremor. J Neural Eng 2012; 9: 046005.
Krack P, Fraix V, Mendes A, Benabid AL, Pollak P. Postoperative management of subthalamic nucleus stimulation for parkinson's disease. Mov Disord 2002; 17 (Suppl 3): S188–97.
Lambert C, Zrinzo L, Nagy Z, Lutti A, Hariz M, Foltynie T, et al. Confirmation of functional zones within the human subthalamic nucleus: patterns of connectivity and sub-parcellation using diffusion weighted imaging. Neuroimage 2012; 60: 83–94.
Lozano AM, Lipsman N. Probing and regulating dysfunctional circuits using deep brain stimulation. Neuron 2013; 77: 406–24.
Lungu C, Malone P, Wu T, Ghosh P, McElroy B, Zaghloul K, et al. Temporal macrodynamics and microdynamics of the postoperative impedance at the tissue-electrode interface in deep brain stimulation patients. J Neurol Neurosurg Psychiatry 2013. Advance Access published on November 11, 2013, doi:10.1136/jnnp-2013-306066.
Maks CB, Butson CR, Walter BL, Vitek JL, McIntyre CC. Deep brain stimulation activation volumes and their association with neurophysiological mapping and therapeutic outcomes. J Neurol Neurosurg Psychiatry 2009; 80: 659–66.
Martens HCF, Toader E, Decré MMJ, Anderson DJ, Vetter R, Kipke DR, et al. Spatial steering of deep brain stimulation volumes using a novel lead design. Clin Neurophysiol 2011; 122: 558–66.
McIntyre CC, Mori S, Sherman DL, Thakor NV, Vitek JL. Electric field and stimulating influence generated by deep brain stimulation of the subthalamic nucleus. Clin Neurophysiol 2004; 115: 589–95.
McIntyre CC, Richardson AG, Grill WM. Modeling the excitability of mammalian nerve fibers: Influence of afterpotentials on the recovery cycle. J Neurophysiol 2002; 87: 995–1006.
Peppe A, Gasbarra A, Stefani A, Chiavalon C, Pierantozzi M, Fermi E, et al. Deep brain stimulation of CM/PF of thalamus could be the new elective target for tremor in advanced Parkinson's Disease? Parkinsonism Relat Disord 2008; 14: 501–04.
Plaha P, Ben-Shlomo Y, Patel NK, Gill SS. Stimulation of the caudal zona incerta is superior to stimulation of the subthalamic nucleus in improving contralateral parkinsonism. Brain 2006; 129: 1732–47.
Pollo C, Vingerhoets F, Pralong E, Ghika J, Maeder P, Meuli R, et al. Localization of electrodes in the subthalamic nucleus on magnetic resonance imaging. J Neurosurg 2007; 106: 36–44.
Rattay F. Analysis of models for external stimulation of axons. IEEE Trans Biomed Eng 1986; 33: 974–77.
Rodriguez-Oroz MC, Rodriguez M, Guridi J, Mewes K, Chockkman V, Vitek J, et al. The subthalamic nucleus in Parkinson's disease: somatotopic organization and physiological characteristics. Brain 2001; 124: 1777–90.
Schaltenbrand G, Wahren W. Atlas for stereotaxy of the human brain. Stuttgart: Thieme, 1977.
Schlaepfer TE, Bewernick BH, Kayser S, Mädler B, Coenen VA. Rapid effects of deep brain stimulation for treatment-resistant major depression. Biol Psychiatry 2013; 73: 1204–12.
Stefurak T, Mikulis D, Mayberg H, Lang AE, Hevenor S, Pahapill P, et al. Deep brain stimulation for Parkinson's disease dissociates mood and motor circuits: a functional MRI case study. Mov Disord 2003; 18: 1508–41.
Temel Y, Kessels A, Tan S, Topdag A, Boon P, Visser-Vandewalle V. Behavioural changes after bilateral subthalamic stimulation in advanced Parkinson disease: a systematic review. Parkinsonism Relat Disord 2006; 12: 265–72.
Thevathasan W, Coyne TJ, Hyam JA, Kerr G, Jenkinson N, Aziz TZ, et al. Pedunculopontine nucleus stimulation improves gait freezing in Parkinson disease. Neurosurgery 2011; 69: 1248–53.
Tripoliti E, Zrinzo L, Martinez-Torres I, Tisch S, Frost E, Borrell E, et al. Effects of contact location and voltage amplitude on speech and movement in bilateral subthalamic nucleus deep brain stimulation. Mov Disord 2008; 23: 2377–383.
Yelnik J, Damier P, Demeret S, Gervais D, Bardinet E, Bejjani BP, et al. Localization of stimulating electrodes in patients with Parkinson disease by using a three-dimensional atlas-magnetic resonance imaging coregistration method. J Neurosurg 2003; 99: 89–99.